

TURBULENT VORTEX SHEDDING FROM A DUAL-STEP CYLINDER: INFLUENCE OF DIAMETER RATIO AND ASPECT RATIO

Chris Morton

Department of Mechanical and Mechatronics Engineering
University of Waterloo
Waterloo, Ontario, Canada, N2L 3G1
cmorton@uwaterloo.ca

Serhiy Yarusevych

Department of Mechanical and Mechatronics Engineering
University of Waterloo
Waterloo, Ontario, Canada, N2L 3G1
syarus@uwaterloo.ca

ABSTRACT

In the present study, the influence of aspect ratio (L/D) and diameter ratio (D/d) on the flow development past a dual-step cylinder is investigated experimentally for $Re_D = 2100$, $1.33 \leq D/d \leq 2.67$, and $0.2 \leq L/D \leq 3$. Experiments are carried out in a water flume facility using Laser Doppler Velocimetry (LDV), Particle Image Velocimetry (PIV), and hydrogen bubble flow visualization. The results show that four distinct vortex shedding regimes can be identified based on changes in large cylinder wake development. Depending on the geometrical parameters of the dual-step cylinder, the wake of the large cylinder may involve (i) vortex shedding at a frequency lower than that expected for a uniform cylinder at the same Reynolds number, (ii) irregular shedding, (iii) vortex shedding at a frequency higher than that for a uniform cylinder, and (iv) suppression of large cylinder vortex shedding. Based on the present results and those from previous studies on relevant geometries, a map of wake regimes for a dual-step cylinder has been constructed.

INTRODUCTION

The present investigation is focused on the flow development over dual-step cylinders. A dual-step cylinder, shown in Fig. 1, consists of a large diameter cylinder (D) of low aspect ratio (L/D) attached coaxially to the mid-span of a small diameter cylinder (d). It is instructive to consider the dual-step cylinder geometry in limiting cases of D/d and L/D . As D/d approaches unity, the dual-step cylinder approaches the geometry of a uniform circular cylinder. On the other hand, for large D/d , the dual-step cylinder resembles a cylinder with two free ends. Hence, it is expected that, depending on the geometrical parameters of the model, the flow development for a dual-step cylinder may be similar to that found for a low aspect ratio uniform cylinder (e.g., Norberg, 1994), a cylinder with free ends (e.g., Inoue &

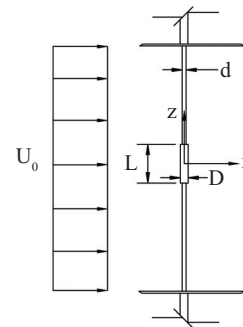


Fig. 1 Experimental arrangement.

Sakuragi, 2008), or a coin-like cylinder (e.g., Zdravkovich et al., 1998).

For uniform circular cylinders mounted between endplates, the frequency of vortex shedding tends to decrease with decreasing aspect ratio for about $L/D < 30$ (Norberg, 1994). For $L/D < 7$, the coherence and strength of the vortex shedding decreases, with regular vortex shedding being replaced by the formation of less coherent wake structures (Norberg, 1994).

Zdravkovich et al. (1989, 1998) and Inoue & Sakuragi (2008) investigated the flow development over uniform cylinders with two free ends. In the laminar vortex shedding regime, Inoue & Sakuragi (2008) found that three wake patterns can occur depending on Re_D and L/D : (i) spanwise vortex shedding, (ii) a steady wake consisting of two counter-rotating streamwise vortices, and (iii) alternate shedding of streamwise vortex pairs from the flat cylinder ends. Zdravkovich et al. (1989) performed experiments for $6000 \leq Re_D \leq 26000$ and $2 \leq L/D \leq 8$. For all models investigated, spanwise vortex shedding occurred in the wake, however, it was intermittent, and the shedding frequency varied with time. Zdravkovich et al. (1998) investigated the flow development over coin-like cylinders for $20000 \leq Re_D \leq 60000$ and

$0.02 \leq L/D \leq 0.9$. The wake was found to be steady and comprised of two counter-rotating vortex pairs, similar to the findings of Inoue & Sakuragi (2008).

Previous investigations on dual-step cylinders (e.g., Williamson, 1992; Morton & Yarusevych, 2012) have shown that vortex shedding occurs in the wake of the small diameter cylinder; however, the large diameter cylinder wake is influenced significantly by the geometrical parameters of the model and the Reynolds number. Williamson (1992) studied the dual-step cylinder wake topology for $Re_d \leq 200$, $D/d = 1.1$ and 1.5 , and $L/d = 0.5$. His results show that periodic vortex dislocations occur downstream of the large cylinder. The frequency of vortex dislocations increases with increasing D/d . Morton & Yarusevych (2012) studied the effect of L/D on the flow development past a dual-step cylinder for $0.2 \leq L/D \leq 17$, $D/d = 2$, and $Re_D = 1050$. They identified the following four distinct flow regimes based on the changes in large cylinder flow topology with L/D : (i) for $L/D > 15$, three vortex shedding cells form downstream of the large cylinder, with the vortex shedding frequency of the central cell being similar to that of a uniform cylinder at the same Reynolds number, (ii) for $8 < L/D \leq 14$, a single vortex shedding cell forms in the wake of the large cylinder whose frequency decreases with decreasing L/D , (iii) for $2 < L/D \leq 6$, the vortex shedding is highly three-dimensional, with less coherent large cylinder vortices deforming significantly in the near wake, and (iv) for $0.2 \leq L/D < 2$, similar to the findings of Williamson (1992) for the laminar vortex shedding regime, vortex dislocations occur downstream of the large cylinder. Morton & Yarusevych (2012) indicated that vortex shedding from the large cylinder could not be identified via flow visualization for this flow regime.

Morton & Yarusevych (2013) investigated the turbulent vortex shedding behind low aspect ratio dual-step cylinders for $1050 \leq Re_D \leq 2100$, $D/d = 2$, and $0.2 \leq L/D \leq 3$. The aspect ratio of the large cylinder was found to have a profound effect on the large cylinder wake development. For higher aspect ratios, $L/D \geq 1$ at $Re_D = 2100$ and $L/D \geq 2$ at $Re_D = 1050$, vortex shedding occurs in the wake of the large and small cylinders at distinct frequencies. For lower aspect ratios, however, vortex shedding in the wake of the large cylinder ceases, and the flow development becomes similar to that observed by Williamson (1992), with vortex dislocations occurring in the large cylinder wake.

The present study is aimed at investigating the effects of both the aspect ratio (L/D) and diameter ratio (D/d) on turbulent wake development of a dual-step cylinder.

EXPERIMENTAL SETUP

Experiments were carried out in a water flume at the University of Waterloo. The cylinder models were mounted between circular endplates (Fig. 1) and placed in a uniform region of the flow. For all dual-step cylinder models, the large cylinder diameter remains fixed in order to maintain constant Re_D through the experiments. Thus, the diameter ratio (D/d) and aspect ratio (L/D) are adjusted by changing the diameter of the small cylinder (d) and the length of the large cylinder (L), respectively.

Experimental measurements on uniform cylinders were also carried out at Reynolds numbers matching that of the large cylinder and each of the small cylinders, i.e., $788 \leq Re_D \leq 2100$.

Flow visualization was performed using the hydrogen bubble technique. Hydrogen bubbles were generated on a $85 \mu\text{m}$ diameter stainless steel wire placed approximately $0.7D$ upstream of the model axis. The flow was illuminated with a conical laser beam generated by passing a laser light source through two consecutive cylindrical lenses. Flow visualization image sequences were obtained with a Photron camera operating at a 100 Hz image acquisition rate.

A Laser Doppler Velocimetry (LDV) system was employed for velocity measurements. Streamwise velocity measurements were acquired at $x/D = 5$, $y/D = 0.75$, and $z/D = 0$. The flow was seeded with $10 \mu\text{m}$ diameter hollow glass spheres, allowing mean data acquisition rates of greater than 50 Hz. For spectral analysis, the velocity data were re-sampled at a fixed frequency of 30 Hz using the sample and hold technique (Adrian & Yao, 1987). The frequency resolution of all spectra analysed is approximately $\pm 0.002 fD/U_0$. Additionally, velocity spectrograms were computed with the same re-sampled velocity signals, with a frequency resolution of $\pm 0.01 fD/U_0$.

Time-resolved Particle Image Velocimetry (PIV) measurements were performed using a LaVision PIV system comprised of a 1024×1024 pixels Photron camera and a high repetition rate Nd:YLF pulsed laser. The seeding material was the same as that used for LDV. Images were acquired at a fixed rate of 100 Hz and processed using DaVis 8 image processing software. For vector processing, interrogation windows of 16×16 pixels with a 50% overlap were chosen based on the recommendations provided by Keane & Adrian (1992).

RESULTS

Vortex shedding in the wake of a dual-step cylinder was investigated experimentally for $Re_D = 2100$, $1.33 \leq D/d \leq 2.67$, and $0.2 \leq L/D \leq 3$. Figure 2 presents streamwise velocity spectra obtained for all models investigated. The results in Fig. 2 illustrate that variations in dominant frequency occur in the wake with both D/d and L/D . For example, consider spectra pertaining to $D/d = 1.6$ (Fig. 2b). The velocity spectrum for $L/D = 3$ shows a broad peak centred on a frequency lower than that expected for a uniform cylinder at the same Reynolds number (Fig. 2b). As the aspect ratio of the large cylinder is decreased to $L/D = 2$ and 1 , the dominant frequency in the large cylinder wake increases, exceeding the vortex shedding frequency for a uniform cylinder (Fig. 2b). Also, the energy content of the corresponding spectral peak increases, indicating increase in coherence of wake structures. A further decrease in the large cylinder aspect ratio below $L/D = 1$, produces a dual peak in the spectrum, with one peak centred at a frequency matching the expected vortex shedding frequency of the small diameter cylinder and the other at a slightly lower frequency, as can be seen in the spectra pertaining to $L/D = 0.5$ in Fig. 2b. At $L/D = 0.2$, the energy content associated with the small cylinder shedding frequency becomes dominant (Fig. 2b). The observed trends can also be seen for other diameter ratios investigated (Fig. 2) and agree with those reported

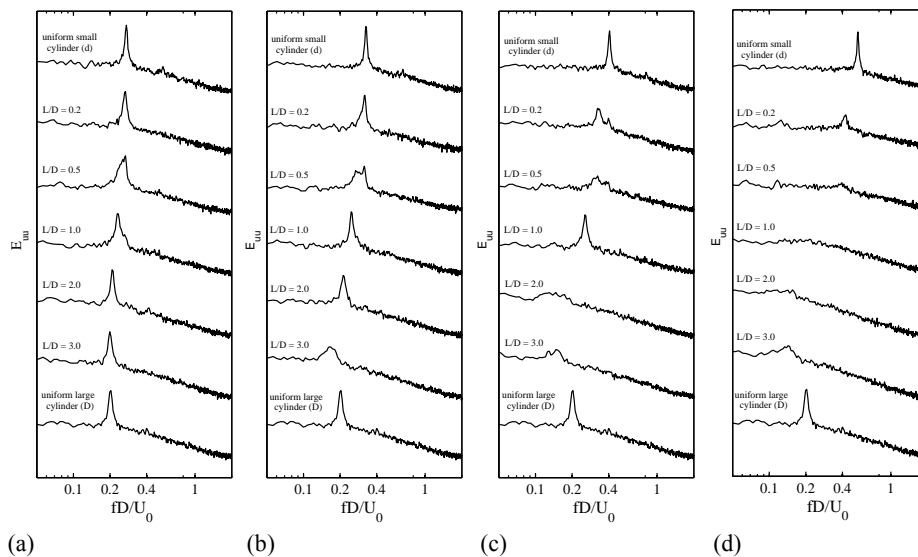


Fig. 2 Wake velocity spectra for (a) $D/d = 1.33$, (b) $D/d = 1.6$, (c) $D/d = 2$, (d) $D/d = 2.67$. Velocity spectra pertaining to uniform cylinders of diameter D and d are included for each D/d investigated. Each velocity spectrum is normalized by the variance of the corresponding velocity signal. The energy content of each velocity spectrum is offset by more than one order of magnitude for clarity.

by Morton & Yarusevych (2012) and Morton & Yarusevych (2013) for dual-step cylinders with $D/d = 2$, $0.2 \leq L/D \leq 3$, and $Re_D = 1050$ and 2100 , respectively.

The changes in velocity spectra seen in Fig. 2 are reflecting changes in the large cylinder wake topology. Through a comparison of the velocity spectra with flow visualization video records and PIV measurements, four distinct large cylinder wake regimes were identified. They are presented in a diagram shown in Fig. 3. The markers in the diagram are used to identify the D/d and L/D values investigated in the present study as well as those investigated by Morton & Yarusevych (2012). The boundaries between different regimes are marked by solid and dashed lines, with the latter drawn based on extrapolation of the present data and results from other relevant studies. For each flow regime, a representative flow visualization image, velocity spectrum, and velocity spectrogram are presented in insets above and below the diagram. In addition, Figs. 4-7 show PIV measurements obtained at the mid-span of the dual-step cylinder models matching the geometries depicted in the insets in Fig. 3.

In the Low Frequency Shedding (LFS) regime, the formation and shedding of vortices from the large cylinder can be identified through flow visualization. A representative visualization image shown in Fig. 3 for $D/d = 1.33$ and $L/D = 3$ shows spanwise vortices shed from the large and small cylinders connecting across the span of the model. The corresponding velocity spectrum shows a well-defined peak associated with the large cylinder vortex shedding frequency, which is slightly less than that expected for a uniform cylinder at the same Reynolds number (Fig. 2a). The energy content associated with the peak is, however, comparable to that of a uniform cylinder, and the representative velocity spectrogram shows only minor variations in the dominant frequency with time. The corresponding mean and instantaneous planar PIV measurements presented in Fig. 4 indicate a similar near wake topology to that expected for a uniform cylinder. Specifically, symmetric mean re-circulation

zones (Fig. 4a) define the vortex formation region located about $2.5D$ downstream of the large cylinder, and alternating shedding of large cylinder vortices is seen in the instantaneous patterns depicted in Figs. 4b-c. The present results indicate that this flow regime persists down to $L/D = 2$ at $D/d = 1.33$ (Fig. 3). Based on the data of Morton & Yarusevych (2012) for a dual-step cylinder at $Re_D = 1050$, shown by open circles in Fig. 3, the boundary of the LFS regime can be extrapolated to higher L/D ratios. Note, the results of Morton & Yarusevych (2012) suggest that for larger L/D , vortex shedding from the large cylinder occurs in three distinct constant frequency cells along the span. This occurs at $L/D \approx 15$ for $D/d = 2$, with the onset of such a topology expected to depend on D/d , L/D , and Re_D . As L/D is decreased below approximately 10, large cylinder vortices start to deform substantially in the near wake and their coherence decreases, eventually leading to irregular shedding.

In the Irregular Shedding (IS) regime, no consistent vortex shedding pattern can be observed in the large cylinder wake. As seen in the corresponding flow visualization image (Fig. 3), distorted spanwise structures forming in the wake of the large cylinder interact with small cylinder vortices at cell boundaries that extend substantially into the small cylinder wake. Within these boundaries, smaller scale roll-up vortices can be seen within the transverse oriented shear layers emanating from each stepwise discontinuity (Fig. 3). The representative velocity spectrum shows a low magnitude, broadened peak, centred at a frequency less than that expected for a uniform cylinder. The velocity spectrogram shows substantial fluctuations in the energy content and frequency with time, indicative of the reduced coherence and varying scale of vortical structures forming in the large cylinder wake. The corresponding PIV results in Fig. 5 show that the vortex formation region (Fig. 5a) expands substantially compared to the LFS regime (Fig. 4a), and the instantaneous flow patterns (Figs. 5b-c) highlight the intermittent nature of the shedding process. Zdravkovich

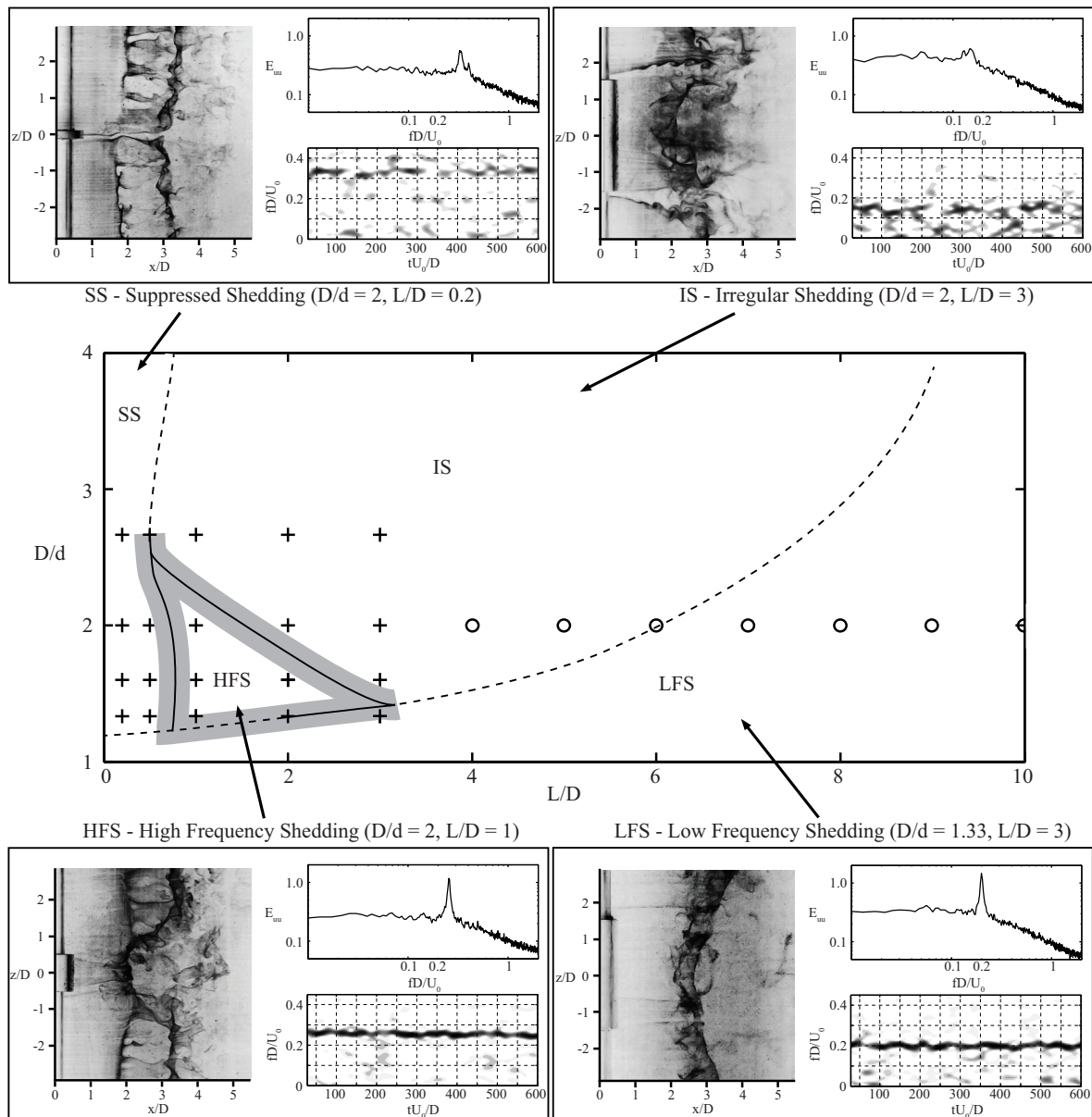


Fig. 3 Diagram of large cylinder wake regimes expected for a dual-step cylinder. The boundaries between different regimes are marked by solid and dashed lines, with the latter drawn based on extrapolation of the present data and results from other relevant studies. The grey area surrounding the boundary lines serves as an estimate of the uncertainty in the boundary location. + symbols represent the L/D and D/d investigated in the present study, o symbols represent a set of geometric parameters investigated by Morton & Yarusevych (2012). Insets show representative flow visualization images, velocity spectra, and spectrograms for each regime at the specified D/d and L/D .

et al. (1989) observed similar wake characteristics for a cylinder with two free ends at $6000 \leq Re_D \leq 26000$ and $2 \leq L/D \leq 8$. Indeed, with increasing D/d , the large cylinder wake topology is expected to approach that of a cylinder with two free ends. Hence, based on the results of Zdravkovich et al. (1989), this flow regime persists at higher D/d than those tested here. Considering previous experiments on cantilevered cylinders (e.g., Fox et al., 1993) and cylinders with other end conditions (e.g., Sheard et al., 2008), the boundary between the IS and LFS regimes is expected to tend asymptotically to $L/D \approx 10$ with increasing D/d .

The High Frequency Shedding regime (HFS) occurs for a narrow range of D/d when the aspect ratio of the large cylinder is within about $1 \leq L/D \leq 2$ (Fig. 3). Rather unexpectedly, the large cylinder vortex shedding becomes intensified in this regime. The representative flow visualization image in Fig. 3 shows a well-defined roll-up of the large cylinder separated shear layer. Analysis of flow visualization video records revealed that, similar to the LFS regime, small and large cylinder vortices interact in the large cylinder wake with vortex connections involving vortex splitting and dislocations. The corresponding velocity spectrum features a narrow

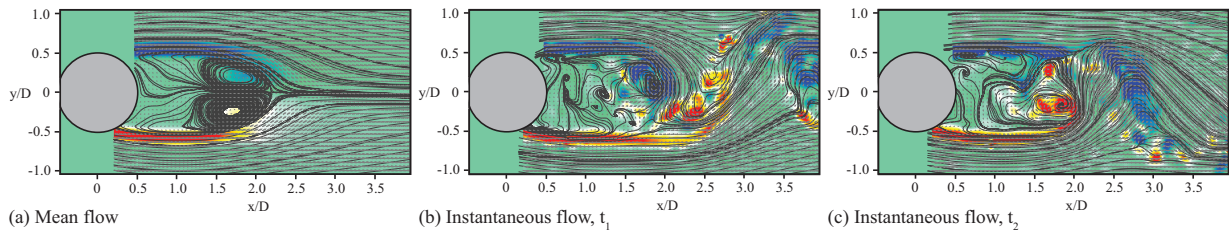


Fig. 4 Planar PIV images at the mid-span of the large cylinder in the LFS regime: $D/d = 1.33$, $L/D = 3$.

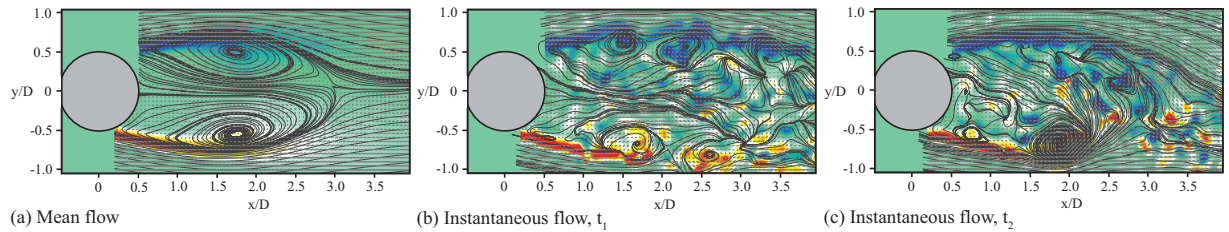


Fig. 5 Planar PIV images at the mid-span of the large cylinder in the IS regime: $D/d = 2.0$, $L/D = 3$.

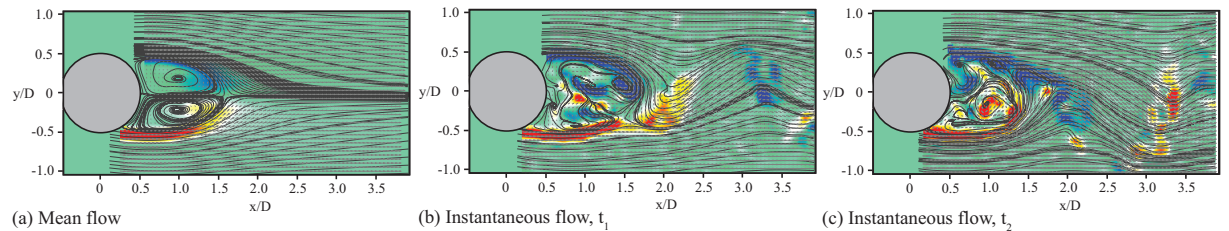


Fig. 6 Planar PIV images at the mid-span of the large cylinder in the HFS regime: $D/d = 2.0$, $L/D = 1$.

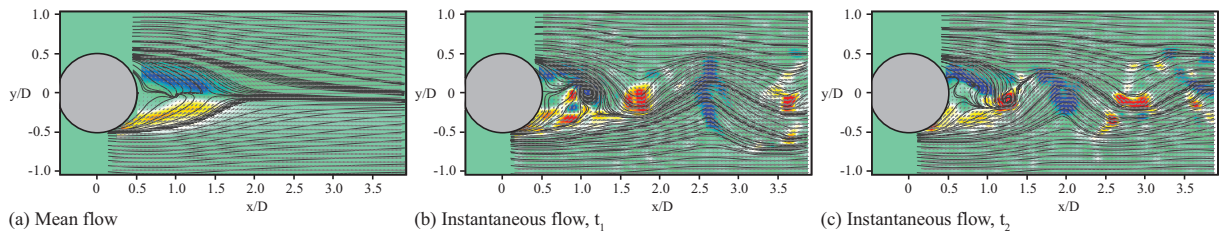


Fig. 7 Planar PIV images at the mid-span of the large cylinder in the SS regime: $D/d = 2.0$, $L/D = 0.2$.

dominant peak, and the velocity spectrogram shows only minor fluctuations in frequency and energy content. However, the shedding frequency is higher than that expected for a uniform circular cylinder, which is a characteristic feature of this flow regime. The PIV results in Figs. 6a-c show planar wake development similar to that found in the LFS regime. However, the formation region is reduced substantially, leading to the reduction in the scale and increase in the frequency of the shed vortices, as expected from uniform cylinder studies (e.g., Williamson, 1996). Since vortex shedding at such low aspect ratios has not been observed on other similar model geometries, e.g., uniform cylinders between endplates, cylinders with two free ends, and cantilevered cylinders, it is speculated that this regime can only be sustained on a dual-step cylinder geometry in the presence of vortex shedding from the small cylinder. The HFS regime is observed over a narrow range of L/D and D/d , and its occurrence is likely related to a specific relative alignment of the boundary layer separation on the large and small

cylinders, which the former reported to vary significantly within $1 \leq L/D \leq 3$ (Morton & Yarusevych, 2013).

For large cylinder aspect ratios below $L/D \approx 1$, shear layers forming on the large cylinder do not roll up into spanwise structures, which is classified as the Suppressed Shedding (SS) regime in Fig. 3. The absence of the shear layer roll-up in the large cylinder wake can be seen in the corresponding flow visualization image in Fig. 3. Analysis of flow visualization video records revealed that small cylinder vortices form vortex connections across the wake of the large cylinder, with the presence of the large cylinder inducing vortex dislocations. The corresponding wake velocity spectrum features a characteristic dual peak. The higher frequency peak is associated with the small cylinder shedding; whereas, the lower frequency peak is due to the passage of vortex connections in the large cylinder wake. As discussed by Morton & Yarusevych (2013), the presence of the large cylinder results in reduced convective velocity of vortex filaments in its wake, which reduces the effective shedding frequency and

leads to vortex dislocations. High amplitude regions associated with two characteristic spectral frequencies can be identified in the corresponding velocity spectrogram in Fig. 3. It should be noted that the dual peak structure becomes difficult to identify in the spectra for lower D/d (Fig. 2), as the two frequencies become more closely spaced with decreasing D/d . Also, at higher D/d , the energy content of the dual peak decreases, as the vortex filaments diffuse and become weaker before reaching the fixed measurement volume in the large cylinder wake. Figures 7a-c show planar PIV results corresponding to the inset images for the SS regime. The absence of recirculating zones in the mean flow field (Fig. 7a) and the instantaneous flow field snapshots in Figs. 7b-c, confirm that the shear layers from the large cylinder do not roll-up into vortical structures. The instantaneous results show smaller-scale vortices in the large cylinder wake that do not originate from the large cylinder separated shear layers, but are footprints of vortex connections between small cylinder vortices, as discussed in detail by Morton & Yarusevych (2013). As D/d increases, for $L/D < 1$, the dual-step cylinder geometry tends to that of a coin-like cylinder with two free ends investigated by Zdravkovich et al. (1998). His results show that, for $L/D < 0.9$, the wake of a coin-like cylinder is steady, similar to the wake of the large cylinder in the SS regime in the present study. Thus, the boundary between the SS and IS regimes can be extrapolated to higher D/d ratios (Fig. 3). Evidently, at sufficiently high D/d , the large cylinder will act as an end plate, preventing small cylinder vortices from connecting across the large cylinder wake and generating a flow field resembling that in Fig. 24 of Williamson (1989). On the other hand, as the diameter ratio decreases towards $D/d = 1$, the influence of the large cylinder on the wake development diminishes, and vortex shedding from the large cylinder is expected to resume, marking the transition to the LFS regime (Fig. 3).

CONCLUSIONS

The turbulent flow development past a dual-step cylinder has been investigated experimentally for $Re_D = 2100$, $1.33 \leq D/d \leq 2.67$, and $0.2 \leq L/D \leq 3$.

The results have shown that the large cylinder wake development can be divided into four distinct flow regimes. Based on the analysis of the present results and those from previous studies on relevant geometries, a comprehensive map is proposed for the identified regimes.

In the Low Frequency Shedding (LFS) regime, which is observed at sufficiently high aspect ratios, spanwise vortex shedding occurs from the large cylinder at a frequency lower than that expected for a uniform cylinder at the same Re_D . At lower D/d , this regime can persist at much lower aspect ratios than those expected for a uniform cylinder or a cylinder with two free ends. However, increasing D/d decreases the coherence of large cylinder vortices, eventually leading to irregular shedding of coherent structures. In this Irregular Shedding (IS) regime, spanwise vortex shedding occurs intermittently, at a frequency lower than that of a uniform cylinder, with the shedding becoming more irregular as L/D decreases. For $L/D \leq 1$, the shedding from the large cylinder ceases, which is classified as the Suppressed Shedding (SS) regime. In this regime, small cylinder vortices connect across the wake of the large cylinder. The presence of the

large cylinder results in reduced convective velocity of the vortex filaments, leading to vortex dislocations. The frequency of dislocations are expected to diminish with decreasing D/d . For a narrow range of geometric parameters ($1 \leq L/D < 2$ and $1.33 \leq D/d \leq 2.0$), well-defined vortex shedding occurs in the large cylinder wake at a frequency higher than that expected for a uniform cylinder. This wake topology is referred to as the High Frequency Shedding (HFS) regime. The bounds of this regime are strongly dependant on D/d and L/D . At such low aspect ratios, the regime itself appears to be unique to the dual-step cylinder geometry due to the presence of highly coherent small cylinder shedding.

REFERENCES

- Adrian, R.J., and Yao, C.S., 1987, "Power spectra of fluid velocities measured by laser Doppler velocimetry," *Experiments in Fluids*, Vol. 5, pp. 17-28.
- Fox T.A., Apelt, C.J., and West, G.S., 1993, "The aerodynamic disturbance caused by the free-ends of a circular cylinder immersed in a uniform flow," *Journal of Wind Engineering and Industrial Aerodynamics*, Vol. 49, pp. 389-400.
- Inoue, O., and Sakuragi, A., 2008, "Vortex shedding from a circular cylinder of finite length at low Reynolds numbers," *Physics of Fluids*, Vol. 20, 033601.
- Keane R.D., Adrian, R.J., 1992, "Theory of cross-correlation of PIV images," *Applied Scientific Research*, Vol. 49, pp. 191-215.
- Morton, C., and Yarusevych, S., 2012, "An experimental investigation of flow past a dual step cylinder," *Experiments in Fluids*, Vol. 52, pp. 69-83.
- Morton, C., and Yarusevych, S., 2013, "Vortex Shedding from Low Aspect Ratio Dual Step Cylinders," Submitted to *Journal of Fluids and Structures*.
- Norberg, C., 1994, "An experimental investigation of the flow around a circular cylinder: influence of aspect ratio," *Journal of Fluid Mechanics*, Vol. 258, pp.287-316.
- Norberg, C., 2003, "Fluctuating lift on a circular cylinder: review and new measurements," *Journal of Fluids and Structures*, Vol. 17, pp. 57-96.
- Prasad, A., and Williamson, C.H.K., 1997, "The instability of the shear layer separating from a bluff body," *Journal of Fluid Mechanics*, Vol. 333, pp. 375-402.
- Sheard, G.J., Thompson, M.C., and Hourigan, K., 2008, "Flow normal to a short cylinder with hemispherical ends," *Physics of Fluids*, Vol. 20, 041701.
- Williamson, C.H.K., 1989, "Oblique and parallel modes of vortex shedding in the wake of a circular cylinder at low Reynolds numbers," *Journal of Fluid Mechanics*, Vol. 206, pp. 579-627.
- Williamson, C.H.K., 1992, "The natural and forced formation of spot-like 'vortex dislocations' in the transition of a wake," *Journal of Fluid Mechanics*, Vol. 243, pp. 393-441.
- Zdravkovich, M. M., Brand, V. P., Mathew, G., and Weston, A., 1989, "Flow past short circular cylinders with two free ends," *Journal of Fluid Mechanics*, Vol. 203, pp. 557-575.
- Zdravkovich M.M., Flaherty A.J., Pahle M.G., Skelthorne I.A., 1998, "Some aerodynamic aspects of coin-Like cylinders," *Journal of Fluid Mechanics*, Vol. 360, pp. 73-84.